SLAC – PUB – 3436
September 1984
(T/E)

PHYSICS AT THE J/ψ AND THE STATUS OF GLUEBALLS*

JACQUES PERRIER

Institute for Particle Physics
University of California
Santa Cruz, California, 95064

and

Stanford Linear Accelerator Center
Stanford University, Stanford, CA 94305

ABSTRACT

Recent results on the J/ψ, $\iota(1440)$, and $\theta(1690)$ from the Crystal Ball, DM2, and Mark III collaborations are presented together with preliminary results on charmonium states from the CERN-ISR R704 experiment. The J/ψ two-body decays into a vector and a pseudoscalar meson are discussed; these results provide information about the quark content of the η and η' and are relevant to models in which these states are mixed with glueballs. New spin-parity determinations of the $\iota(1440)$ and $\theta(1690)$ are presented, as well as several recent branching ratio measurements including evidence for the decay $\theta(1690) \to \pi^+\pi^-$.

Invited talk presented at the International Conference "Physics in Collision IV," Santa Cruz, California, August 22-24, 1984.

---

* Work supported in part by the Department of Energy, contract DE-AC03-76SF00515 (SLAC) and by contract number DE – AM03-76SF00034.

1. INTRODUCTION

The number of physics results produced by the different experiments that have recently taken data at the J/ψ energy in e^+e^- storage rings is so large that it is impossible to review all of them in a short amount of time. For this reason, I have selected a limited number of topics:

- Measurements of the $J/\psi \rightarrow$ Vector+Pseudoscalar branching ratios (Mark III); particularly interesting numbers which can be used to evaluate the non-strange and strange quark content of the η and η' pseudoscalar mesons.

- $\iota(1440)$: I will present a new spin-parity analysis of the $J/\psi \rightarrow \gamma K_S K^{\pm}\pi^{\mp}$ channel (Mark III) together with recent results on the radiative decay modes $\iota \rightarrow \gamma\rho^0$, $\iota \rightarrow \gamma\phi$, and $\iota \rightarrow \gamma\omega$ (Crystal Ball, DM2, Mark III).

- $\theta(1690)$: The result of a recent spin-parity analysis of the $J/\psi \rightarrow \gamma K^+K^-$ channel , several new upper limits and branching ratio measurements are presented (Crystal Ball, DM2, Mark III). Evidence for its $\pi^+\pi^-$ decay mode has been obtained for the first time (Mark III).

- $\chi(3510)$, $\chi(3555)$, and $\eta_c(2980)$: The last CERN-ISR experiment (R704) has measured the $p\bar{p}$ partial width of the $\chi(3510)$ and $\chi(3555)$, and the product of branching ratios $B(\eta_c \rightarrow p\bar{p}) \times B(\eta_c \rightarrow \gamma\gamma)$.

Large data samples were required to obtain the preceding results: Crystal Ball collected 2.2×10^6 J/ψ's, DM2: 8×10^6 of which 4.4×10^6 were analyzed at the time of this talk, and Mark III: 2.7×10^6.

The four diagrams believed to be mainly responsible for the decay of the J/ψ are shown in Fig. 1. Their relative contributions to the J/ψ width are approximately in the ratios 65:30:5:1.

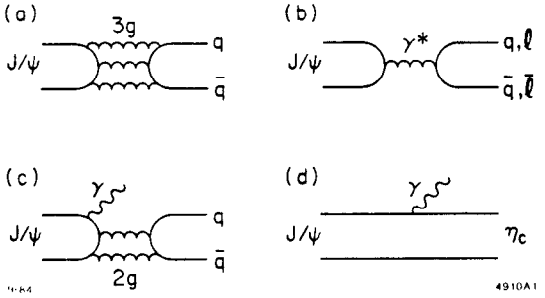

Figure 1. a) Three gluon annihilation. b) Electromagnetic decay proceeding via $c\bar{c}$ annihilation into one photon. c) Electromagnetic decay into a final state of one photon and two gluon color singlet. d) Magnetic dipole transition to the $\eta_c(2980)$.

2. $J/\psi \to$ VECTOR + PSEUDOSCALAR DECAYS

The branching ratios for the decay $J/\psi \to$Vector+Pseudoscalar, recently measured by the Mark III, are given in Tab.1. Several new decays are observed, including two purely electromagnetic (isospin violating) modes, $\rho^0\eta$ and $\omega\pi^0$. The 3-gluon and the single-photon annihilations (Fig. 2a and Fig. 2b) are the two lowest order processes that contribute to these decays. In the following, possible contributions from doubly disconnected diagrams, like the one shown in Fig. 2c where an $s\bar{s}$ pair recoils against a non-strange pair, will be neglected (OZI rule[1]). This assumption is justified by the observation of the $J/\psi \to \omega f$ and $J/\psi \to \phi f'$ decay modes and the absence of $J/\psi \to \omega f'$ and $J/\psi \to \phi f$. The suppression of the doubly disconnected diagrams is also apparent in Tab. 1; the branching ratio for $\phi\pi^0$ is much smaller than that for $\omega\pi^0$.

Table 1. $J/\psi \to V + P$ branching ratios (preliminary). Upper limits are given at the 90% confidence level; first measurements are shown in italics.

Decay Mode	Branching Ratios ($\times 10^{-3}$)
$\rho\pi$	$13.3 \pm 0.2 \pm 2.2$
$K^{*+}K^- + c.c.$	$5.1 \pm 0.1 \pm 0.5$
$K^{*0}\bar{K}^0 + c.c.$	$4.1 \pm 0.1 \pm 0.5$
$\omega\eta$	*$1.9 \pm 0.2 \pm 0.3$*
$\omega\eta'$	*$0.37 \pm 0.09 \pm 0.07$*
$\phi\eta$	$0.68 \pm 0.06 \pm 0.09$
$\phi\eta'$	*$0.37 \pm 0.06 \pm 0.06$*
$\rho^0\eta$	*$0.17 \pm 0.02 \pm 0.04$*
$\rho^0\eta'$	*< 0.1*
$\omega\pi^0$	*$0.67 \pm 0.06 \pm 0.11$*
$\phi\pi^0$	*< 0.013*

In this picture, the quark content of the vector and pseudoscalar mesons are fully correlated. Then, we expect, assuming the vector mesons to be ideally mixed, the partial width $\Gamma(J/\psi \to \omega\eta)$ and $\Gamma(J/\psi \to \phi\eta)$ to be respectively proportional to the non-strange, X_η^2, and strange, Y_η^2, quark content[2] of the η. Thus, the $J/\psi \to V + P$ decays allow us to determine the quark content of the η and η' —a step towards an understanding of the pseudoscalar masses and mixing angle.

The $J/\psi \to V + P$ amplitudes can be expressed in terms of

$g =$ SU(3) symmetric strong amplitude

$e =$ Electromagnetic amplitude.

Their contributions to a specific channel are obtained through a standard SU(3) calculation[3] that gives the result shown in Tab. 2. The known SU(3) violation has been taken into account by a pure octet SU(3) breaking term. This is equivalent to reducing g by a fixed amount h

for each strange quark in the final state and to multiplying the electromagnetic amplitude contributions, which are proportional to the quark magnetic moment μ, by different functions of $x = \frac{\mu_s}{\mu_u} \simeq \frac{m_u}{m_s}$, where m_s and m_u are the strange and non-strange quark masses.

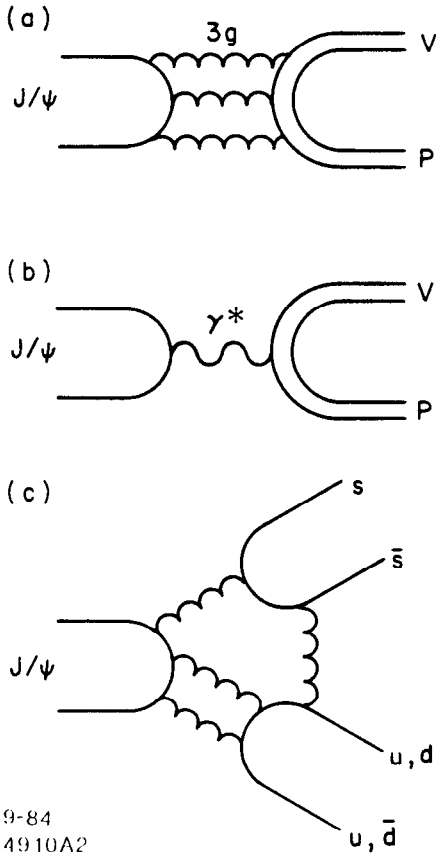

Figure 2. Main contributions to the $J/\psi \to V + P$ decays: a) 3-gluon and b) single-photon annihilation. Neglected contributions: c) doubly disconnected diagrams.

As the $J/\psi \to \rho^0\pi^0$ and $J/\psi \to \omega\eta$ amplitudes are identical up to a coefficient X_η, after phase space correction, the ratio of their branching ratios[4] is

$$\frac{B(J/\psi \to \omega\eta)}{B(J/\psi \to \rho^0\pi^0)} = X_\eta^2. \tag{1}$$

Similarly,

$$\frac{B(J/\psi \to \rho^0\eta)}{B(J/\psi \to \omega\pi^0)} = X_\eta^2. \tag{2}$$

The values of X_η^2, $X_{\eta'}^2$, and $Y_\eta^2/Y_{\eta'}^2$ derived from (1) and (2) and similar equations are given in Tab. 3. The X^2 values obtained from the 3-gluon annihilation dominated decays, $\rho^0\pi^0$, $\omega\eta$, and $\omega\eta'$, are in good agreement with those obtained from the purely electromagnetic decays, $\omega\pi^0$, $\rho^0\eta$, and $\rho^0\eta'$.

Fitting the measured branching ratios with the set of amplitudes given in Tab. 2, we can determine all of the parameters: $|g|$, $|h|$, $|e|$, ϕ(relative phase between (g, h) and e), the X's, and the Y's. The result is given in Tab. 4 and presented in Fig. 3a and Fig. 3b.

Table 2. $J/\psi \to V + P$ amplitudes.

Decay Mode	Amplitude
$\rho^+\pi^-;\rho^0\pi^0;\rho^-\pi^+$	$g \quad +e$
$K^{*+}K^-;K^{*-}K^+$	$g \quad -h+e\cdot(2-x)$
$K^{*0}\bar{K}^0;\bar{K}^{*0}K^0$	$g \quad -h-2e\cdot(\frac{1+x}{2})$
$\omega\eta$	$(g \quad +e)X_\eta$
$\omega\eta'$	$(g \quad +e)X_{\eta'}$
$\phi\eta$	$(g-2h-2e\cdot x)Y_\eta$
$\phi\eta'$	$(g-2h-2e\cdot x)Y_{\eta'}$
$\rho^0\eta$	$3eX_\eta$
$\rho^0\eta'$	$3eX_{\eta'}$
$\omega\pi^0$	$3e$
$\phi\pi^0$	0

Table 3. Quark Content of the η and η' determined from simple ratios. The upper limit is given at the 90% confidence level.

Ratio	Coefficient
$\frac{\omega\eta}{\rho^0\pi^0}$	$X_\eta^2 = 0.48 \pm 0.11$
$\frac{\rho^0\eta}{\omega\pi^0}$	$X_\eta^2 = 0.28 \pm 0.09$
$\frac{\omega\eta'}{\rho^0\pi^0}$	$X_{\eta'}^2 = 0.12 \pm 0.04$
$\frac{\rho^0\eta'}{\omega\pi^0}$	$X_{\eta'}^2 < 0.21$
$\frac{\phi\eta'}{\phi\eta}$	$\frac{Y_{\eta'}^2}{Y_\eta^2} = 0.73 \pm 0.19$

Table 4. Result of the global fit.

$\lvert g\rvert = 1.18 \pm 0.06$	$\lvert X_\eta\rvert = 0.64 \pm 0.06$
$\lvert h\rvert = 0.26 \pm 0.07$	$\lvert Y_\eta\rvert = 0.84 \pm 0.12$
$\lvert e\rvert = 0.14 \pm 0.02$	$\lvert X_{\eta'}\rvert = 0.34 \pm 0.05$
$\phi = 1.30 \pm 0.14$	$\lvert Y_{\eta'}\rvert = 0.72 \pm 0.12$

The parameter $x = \frac{\mu_s}{\mu_u}$ was fixed at 0.62[5]. A 15% change of its value does not affect the result significantly. Note that the measured SU(3) breaking $|h|/|g|$ is equal to 22% and that the relative contribution of the single photon and 3-gluon annihilation diagrams is $|e|/|g| \simeq 12\%$. Adding the non-strange and strange quark contents, we get

$$X_\eta^2 + Y_\eta^2 = 1.1 \pm 0.2$$
$$X_{\eta'}^2 + Y_{\eta'}^2 = 0.63 \pm 0.18. \qquad (3)$$

The X's and Y's can also be determined from the radiative decay widths of the vector mesons and the two-gamma widths of the pseudoscalar mesons;[2,6] these constraints are shown in Fig. 3c and Fig. 3d.

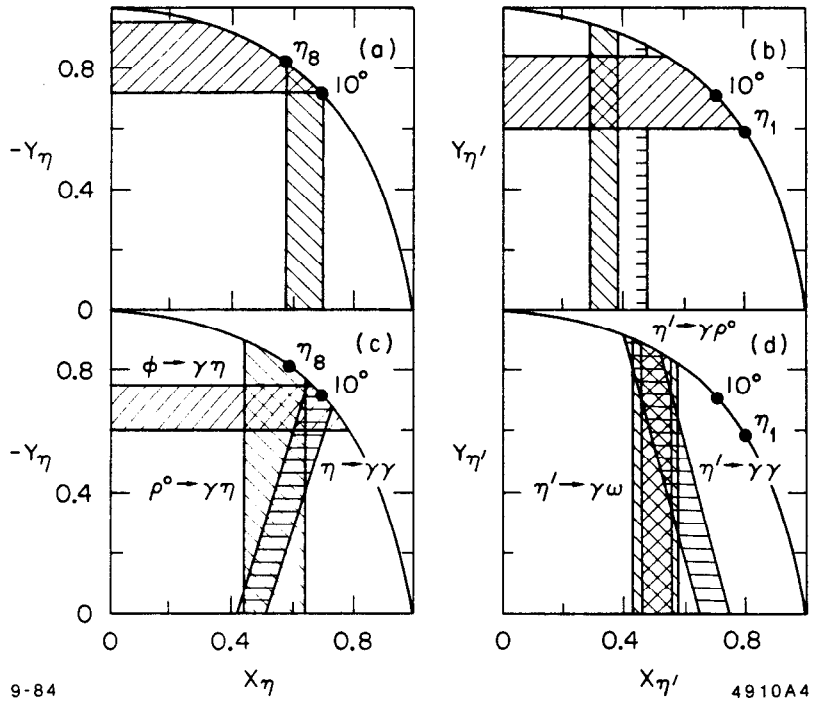

Figure 3. Constraints on X and Y : a) and b) from J/ψ direct decays c) and d) from radiative transitions. $\eta_1(\eta_8)$ shows the quark content expected for a pure singlet η' (octet η). The 10° pseudoscalar mixing angle predictions are also shown.

Although both determinations agree on the η quark contents, there seems to be a disagreement on the value of $|X_{\eta'}|$. However, each one of the three evaluations of $|X_{\eta'}|$—derived respectively from the $\eta' \to \gamma\rho^0$, $\eta' \to \gamma\omega^0$, and $\eta' \to \gamma\gamma$ partial widths—depends upon one number, $\Gamma(\eta' \to \gamma\gamma)$, which was used in the calculation of the η' total width.[6] Thus, if $\Gamma(\eta' \to \gamma\gamma)$ were to change by 25%, the results would agree.

The usual 10° pseudoscalar mixing angle corresponds to $|X_{\eta'}| \simeq \frac{1}{\sqrt{2}}$, value inconsistent with both the radiative transition and the J/ψ decay constraints. As the strange and non-strange quark contents of the η' do not add up to one, it can be mixed with a third pseudoscalar. If, as suggested in some theoretical models, it is the iota, the decays $J/\psi \to \omega\iota$ or $J/\psi \to \phi\iota$ or both should be observed. The iota radiative decay widths, which depend strongly on its quark content, provide another check of this possible mixing.

3. IOTA (1440)

The present experimental status of the $\iota(1440)$ is summarized in Tab. 5. Although the new mass and branching ratio determinations agree with the previous measurements, the width appears to be significantly larger. If a "δ-cut", $m(K\bar{K}) \leq 1.125$ GeV, is applied to the Mark III data, the ι mass decreases by about 20 MeV.

The $K\bar{K}\pi$ effective mass spectra observed in J/ψ radiative decays are shown in Fig. 4a and Fig. 4b. They are characterized by a huge iota signal and very little background, allowing a definitive spin-parity determination.

Table 5. $\iota(1440)$ present experimental status. New measurements appear in italics.

Collaboration	Decay Mode	Mass (MeV)	Width (MeV)	$B(J/\psi \to \gamma\iota)\times$ $B(\iota \to K\bar{K}\pi)$
Mark II[7]	$K_S K^{\pm}\pi^{\mp}$	1440^{+10}_{-15}	50^{+30}_{-20}	$(4.3 \pm 1.7)10^{-3}$
Crystal Ball[8]	$K^+K^-\pi^0$	1440^{+20}_{-15}	55^{+20}_{-30}	$(4.0 \pm 0.7 \pm 1.0)10^{-3}$
Mark III	$K_S K^{\pm}\pi^{\mp}$	*1456 ± 10*	*95 ± 7*	*(5.0 ± 0.5 ± 0.7)10⁻³*
	$K^+K^-\pi^0$	*1460 ± 10*	*103 ± 10*	
DM2[9]	$K_S K^{\pm}\pi^{\mp}$	*1474 ± 15*	*76 ± 16*	

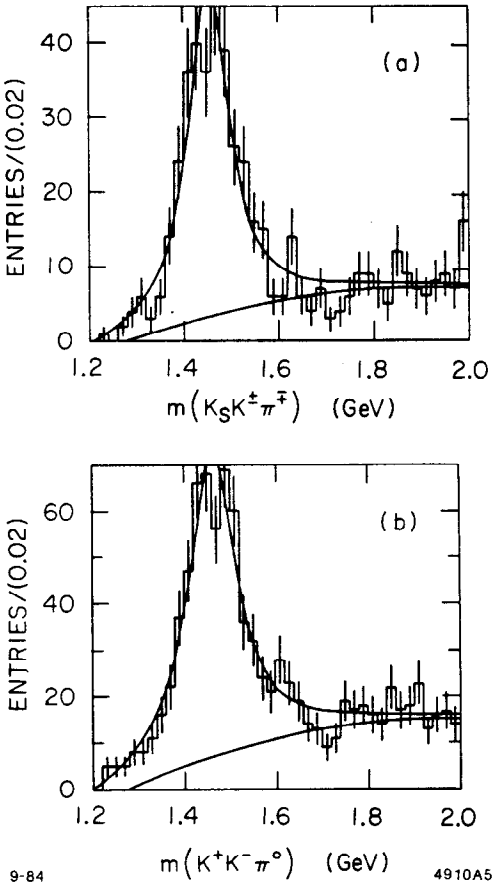

Figure 4. $J/\psi \to \gamma K\bar{K}\pi$: $K\bar{K}\pi$ effective mass spectrum (Mark III).

3.1 Spin and Parity

Some time ago, the Crystal Ball performed a partial-wave analysis of the $K^+K^-\pi^0$ system which included five contributions:[8]

$$\begin{aligned} &\iota \to \delta\pi && (J^P = 0^-, 1^+) \\ &\iota \to K^*\bar{K} + c.c. && (J^P = 0^-, 1^+) \\ &\iota \to K\bar{K}\pi && \text{(phase space)} \end{aligned}$$

The spin parity assignment 0^- was preferred over 1^+, and at the 90% confidence level

$$\frac{B(\iota \to \delta\pi)}{B(\iota \to K^*\bar{K} + c.c.) + B(\iota \to \delta\pi)} > 0.75,$$

where $\delta \to K\bar{K}$. As $B(\delta \to \eta\pi)/B(\delta \to K\bar{K}) \simeq 0.23 - 1.3$,[10] the decay sequence $J/\psi \to \gamma\iota$, $\iota \to \delta\pi$, $\delta \to \eta\pi$ should be observed. The Mark III does not and quotes the following upper limit:

$$B(J/\psi \to \gamma\iota) \cdot B(\iota \to \delta^{\pm}\pi^{\mp}) \cdot B(\delta^{\pm} \to \eta\pi^{\mp}) < 3.9 \times 10^{-4} \text{ at 90\% } C.L.,$$

to be compared with the expected 6×10^{-4} to 3×10^{-3}.

Because of the different assumptions which went into the partial-wave analysis, a spin-parity determination which measures J^P with no assumptions about the two-body decay properties of the iota and gives visual evidence supporting the J^P assignment is desirable. Such an analysis has been performed by Mark III; the Berman-Jacob technique[11] used compares the distributions of the following angles (see Fig. 5):

- θ_γ = angle between the beam and radiative photon directions
- β = angle between the normal to the iota decay plane and the iota direction in its center of mass system
- α = azimuthal angle of the normal to the iota decay plane in the iota center of mass system with respect to the iota production plane

to the predicted distributions given in Tab. 6.

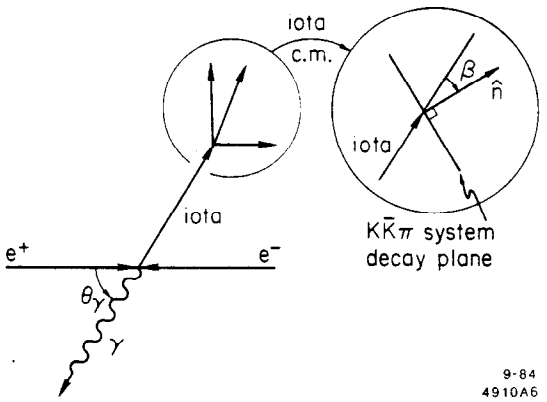

Figure 5. The angles used in the iota J^P analysis.

Table 6. Predicted angular distributions. The 1^+ and 1^- predictions have been integrated over α.

Spin-Parity	Angular Distribution
0^-	$1 + \cos^2\theta_\gamma$; uniform in $\cos\beta$ and α
1^+	$(1 + \cos^2\theta_\gamma)\sin^2\beta + X^2 \cdot \sin^2\theta_\gamma(1 + \cos^2\beta)$
1^-	$(1 + \cos^2\theta_\gamma)\cos^2\beta + X^2 \cdot \sin^2\theta_\gamma \sin^2\beta$

The 1^+ prediction depends upon one unknown parameter $X = \frac{A_1}{A_0}$, where A_0 and A_1 are the helicity 0 and 1 production amplitudes of the iota. For the particular value $X^2 = 2$, the distribution of $\cos\beta$ is uniform, identical to that predicted for a $J^P = 0^-$. However, in this

case, the θ_γ distributions are very different: $1+\frac{3}{2}\sin^2\theta_\gamma$ for $J^P = 1^+$ compared to $1+\cos^2\theta_\gamma$ for $J^P = 0^-$. The distribution of $\cos\beta$, shown in Fig. 6 with the MonteCarlo acceptance, is uniform and therefore compatible with a $J^P = 0^-$ assignment or 1^+ if $X^2 = 2$. The spin-parity 0^- is obviously preferred by the $\cos\theta_\gamma$ distribution (Fig. 6c and Fig. 6d). More quantitatively, the full spin-parity analysis, which is performed in the three dimensional space $(\theta_\gamma, \beta, \alpha)$, gives the following ratios of likelihood values:

$$\frac{\mathcal{L}(1^+)}{\mathcal{L}(0^-)} \simeq e^{-8} \qquad \frac{\mathcal{L}(1^-)}{\mathcal{L}(0^-)} \simeq e^{-13}$$

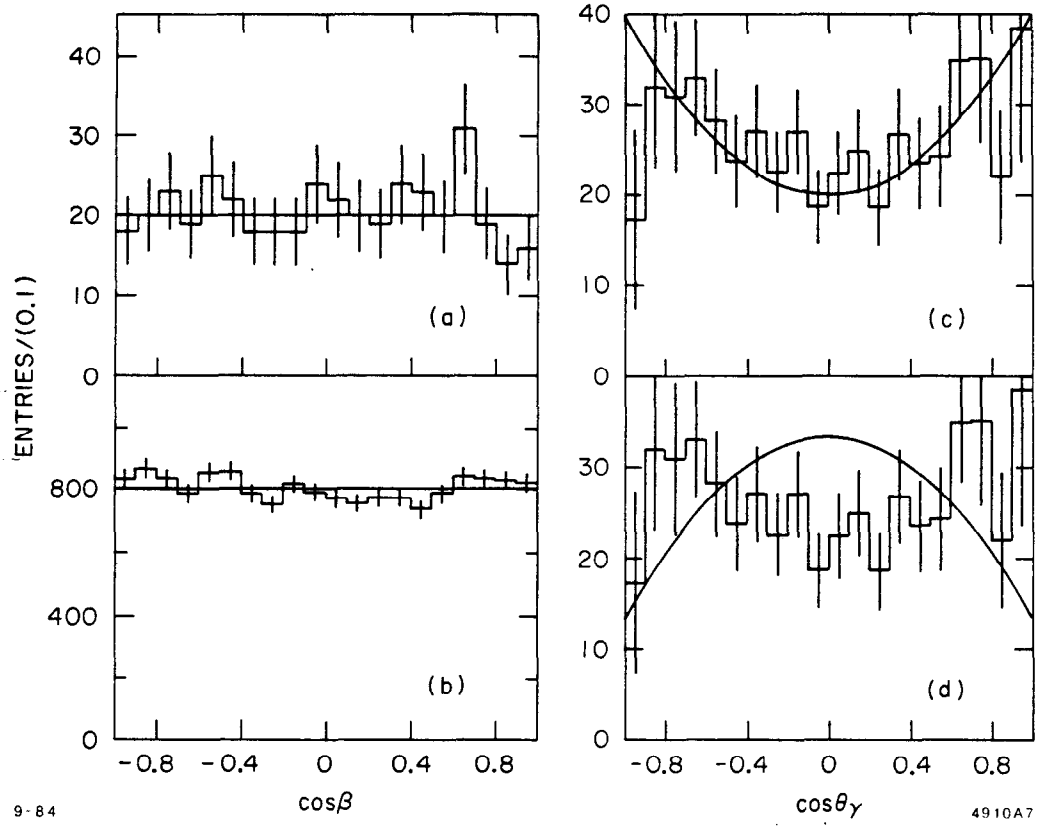

Figure 6. $J/\psi \to \gamma\iota, \iota \to K_S K^\pm\pi^\pm$: a) Distibution of $\cos\beta$ b) Monte Carlo acceptance c) Distribution of $\cos\theta_\gamma$ and the 0^- prediction d) Distribution of $\cos\theta_\gamma$ and the 1^+ prediction (Mark III).

3.2 $\iota \to \gamma V$ Radiative Decays

The radiative decay widths probe the quark content of the iota, as they do for the η and η' pseudoscalar mesons.[12]

- $\iota \to \gamma\rho^0$

Three experiments have looked for the iota in the double radiative decay channel $J/\psi \to \gamma X$, $X \to \gamma\rho^0$. The $\gamma\rho^0$ effective mass distributions are shown in Fig. 7. The spectrum has two main features: a huge narrow η' peak and a relatively broad structure around 1400 MeV, particularly visible in the Mark III and Crystal Ball[13] data. There is some excess of events on the lower mass side of the 1400 MeV structure which might be due to the presence of

$J/\psi \to \gamma f(1270)$ or $J/\psi \to \gamma\eta(1275)$ decays. The parameters of this structure (Mark III),

$$\begin{aligned} \text{mass} &= 1434 \pm 20 \quad \text{MeV} \\ \text{width} &= 133 \pm 50 \quad \text{MeV}, \end{aligned}$$

are the result of a three Breit-Wigner fit where the parameters of the first two were fixed at those of the η' and $f(1270)$. The branching ratio $B(J/\psi \to \gamma X(1400)) \times B(X(1400) \to \gamma\rho^0)$ is given in Tab. 7. These values vary slightly when the $\eta(1275)$ parameters are used instead of those of the f(1270). Although its mass and width are very similar to the iota parameters, a spin-parity determination is required to definitively identify the signal. Unfortunately, the present amount of data does not allow this type of analysis. But the consistency between the observed angular distributions and those predicted for a 0^- state can be checked. The angles that describe the decay are defined in Fig. 8. The observed distributions are consistent with a $J^P = 0^-$ assignment (see Fig. 9.): $1 + \cos^2\theta$ for θ_{γ_1}, uniform in $\cos\theta_{\gamma_2}$ and $\sin^2\theta$ for θ_π. If we attribute the signal to the iota, using $\Gamma_{\text{tot}}(\iota) = 100 \pm 10$ MeV, we get the substantial partial width $\Gamma(X(1400) \to \gamma\rho^0) = (2 \pm 1) \times B(X(1400) \to K\bar{K}\pi)$ MeV. In this case, the iota contains probably a substantial amount of light non-strange quarks.

- $\iota \to \gamma\phi$ and $\iota \to \gamma\omega$

These two decay modes have been looked for by Mark III. The absence of a signal implies the following 90% C.L. upper limits

$$B(J/\psi \to \gamma\iota) \cdot B(\iota \to \gamma\phi) < 2.1 \times 10^{-4}$$

$$B(J/\psi \to \gamma\iota) \cdot B(\iota \to \gamma\omega) < 2.3 \times 10^{-4}$$

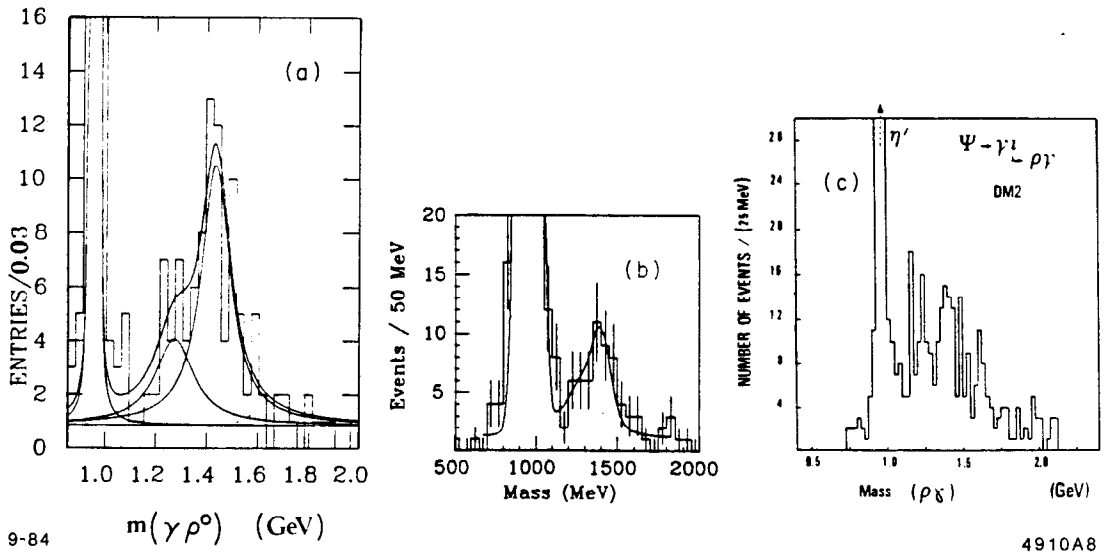

Figure 7. $J/\psi \to \gamma X, X \to \gamma\rho^0$: $\gamma\rho^0$ effective mass distribution. The continuous line is the result of a fit to three Breit-Wigners and a linear background. a) Mark III b) Crystal Ball c) DM2.

Table 7. $J/\psi \to \gamma X(1400), X(1400) \to \gamma\rho^0$ branching ratio. The mass and width of the 1400 MeV structure were respectively fixed at 1440 MeV and 55 MeV in the Crystal Ball fit.

Collaboration	$B(J/\psi \to \gamma X(1400))$ $\times B(X(1400) \to \gamma\rho^0)$
Crystal Ball[13]	$(0.88 \pm 0.28 \pm 0.15)10^{-4}$
Mark III	$(1.1 \pm 0.24 \pm 0.25)10^{-4}$

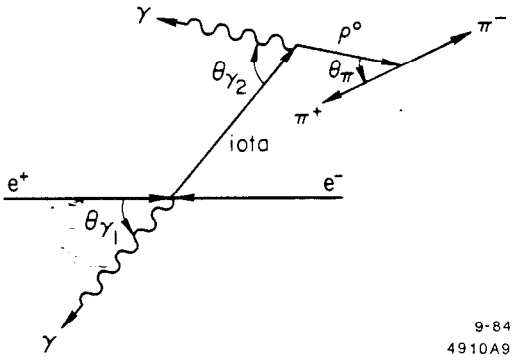

Figure 8. Angles describing the decay sequence $J/\psi \to \gamma X, X \to \gamma\rho^0$.

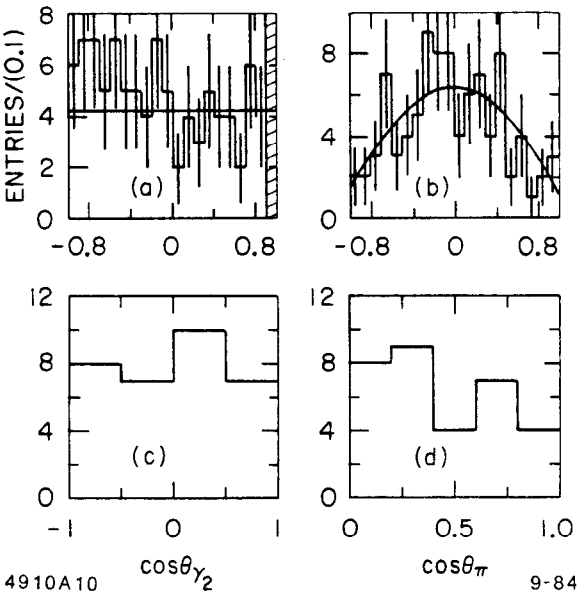

Figure 9. Angular distributions in the iota region. a) and b) Mark III (Mass range: 1300 to 1600 MeV) c) and d) Crystal Ball (mass range: 1350 to 1550 MeV). Note that the $\cos\theta_\pi$ distribution from Crystal Ball is plotted from 0 to 1.

4. THETA(1690)

The present status of the $\theta(1690)$ is summarized in Tab. 8. The new results, in particular the evidence obtained for the $\theta(1690) \to \pi^+\pi^-$ decay mode, should help to understand its nature.

4.1 Spin and Parity

Because it decays into two spinless mesons, the parity and charge conjugation of the $\theta(1690)$ are both equal to $(-1)^L$. Its production in J/ψ radiative decays implies $C = +1$. Therefore, its allowed J^P assignments are $0^{++}, 2^{++}, 4^{++}, \ldots$. The full spin-parity analysis of the $J/\psi \to \gamma\theta(1690), \theta(1690) \to K^+K^-$ decay channel, performed by Mark III , prefers the 2^+ assignment over 0^+ at the 99.9% confidence level.[16,17] The K^+K^- effective mass distribution is shown in Fig. 10; the $f'(1525)$ and the $\theta(1690)$ peaks are well separated.

Table 8. $\theta(1690)$ present experimental status. New measurements appear in italics. Upper limits are given at the 90% confidence level.

Collaboration	Decay mode	mass (MeV)	width (MeV)	$B(\psi \to \gamma\theta) \times B(\theta \to X)$
Crystal Ball[13,14]	$\eta\eta$	1670 ± 50	160 ± 80	$(3.8 \pm 1.6)10^{-4}$
	$\eta\eta'$			$< 2.1\ 10^{-4}$
	$\pi\pi$			$< 6\ 10^{-4}$
Mark III	K^+K^-	*1720 ± 10*	*130 ± 20*	*(4.8 ± 0.6 ± 0.9) 10^{-4}*
	$\pi^+\pi^-$	*1713 ± 15*	–	*(1.6 ± 0.4 ± 0.3) 10^{-4}*
	$\rho^0\rho^0$			*< 2.0 10^{-4}*
	$K\bar{K}\pi$			*< 2.5 10^{-4}*
	$K^+K^-\pi^+\pi^-$			*< 1.0 10^{-4}*
Mark II[15]	K^+K^-	1708 ± 30	156 ± 60	$(6.0 \pm 0.9 \pm 2.5)\ 10^{-4}$
	$\pi\pi$			$< 3.2\ 10^{-4}$
DM2[9]	K^+K^-	*1718 ± 29*	*233 ± 75*	

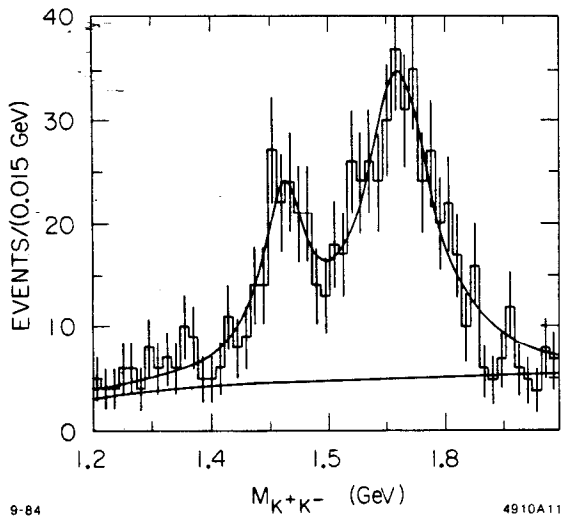

Figure 10. $J/\psi \to \gamma K^+K^-$: K^+K^- effective mass distribution (Mark III).

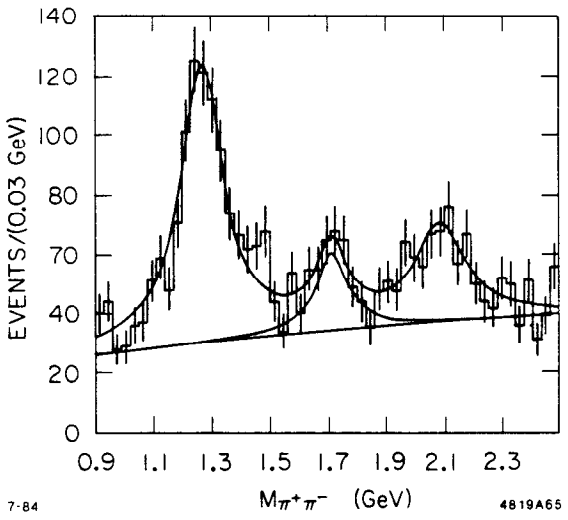

Figure 11. $J/\psi \to \gamma\pi^+\pi^-$: $\pi^+\pi^-$ effective mass distribution (Mark III).

4.2 $\theta(1690) \to \pi^+\pi^-$

The $\pi^+\pi^-$ effective mass distribution, shown in Fig. 11, reveals the presence of two additional structures above the $f(1270)$. The fit performed includes three incoherent Breit-Wigners. The first one has its parameters fixed at those of the $f(1270)$, and the Γ of the second one is set at 130 MeV, the measured $\theta(1690)$ width. The mass of the second peak is found to be 1713 ± 15 MeV, consistent with the $\theta(1690)$ mass. The signal can not be definitively attributed to the $\theta(1690)$ unless a spin and parity analysis is performed. Yet, the angular distributions are similar in the $\pi\pi$ and KK channels. Using the helicity amplitude ratios found in the spin-parity analysis of the $J/\psi \to \gamma K^+K^-$ channel, one finds that

$$B(J/\psi \to \gamma\theta(1690)) \cdot B(\theta(1690) \to \pi^+\pi^-) = (1.6 \pm 0.4 \pm 0.3)10^{-4}$$

Because of the possible interference between the $f(1270)$ and $\theta(1690)$ amplitudes (and perhaps the observed third structure), the true branching ratio might be smaller.[15]

The parameters of the third structure,

$$\begin{aligned} \text{mass} &= 2086 \pm 15 \text{ MeV} \\ \text{width} &= 210 \pm 63 \text{ MeV}, \end{aligned}$$

agree with those of the $h(2030)$. However, its branching ratio,

$$B(J/\psi \to \gamma X(2100)) \times B(X(2100) \to \pi^+\pi^-) = (3.0 \pm 0.5 \pm 0.6)10^{-4},$$

is quite large for a $J^P = 4^+$ state, which is not expected to be strongly produced in the J/ψ radiative decays.

5. RECENT RESULTS ON CHARMONIUM STATES

Finally, I would like to present preliminary results on the $\chi(3510)$, $\chi(3555)$, and $\eta_c(2980)$ states from the last CERN-ISR experiment,[18] whose setup is shown in Fig. 12. The CERN complex is used to produce an intense $\bar{p}$ beam in which $\frac{\Delta p}{p}$ is reduced to $\pm 5 \times 10^{-4}$ by the CERN-ISR stochastic cooling system. A high luminosity, 3×10^{30} cm^{-2}s^{-1}, is achieved by the use of a hydrogen molecular beam target. The detector consists of a two-arm non-magnetic spectrometer with good γ/π^0 and $e^{\pm}/\pi^{\pm}$ separations. Its geometrical acceptance for two photons (electrons) is $\simeq 12\%$.

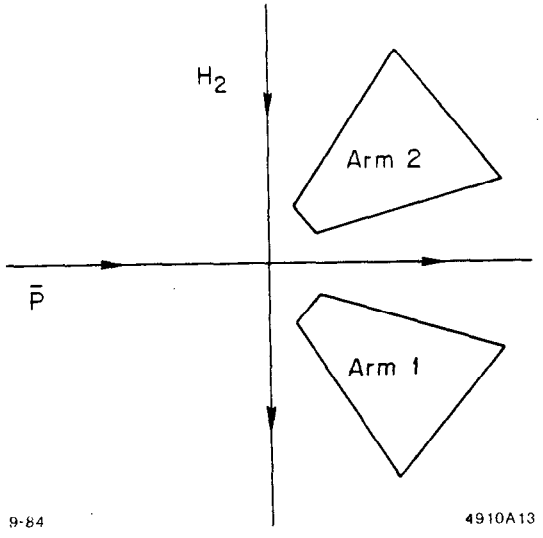

Figure 12. Schema of the CERN R704 experiment.

The following formation/decay sequences were looked for:

- $p\bar{p} \rightarrow J/\psi \rightarrow e^+e^-$
- $p\bar{p} \rightarrow \chi(3510)$ or $\chi(3555) \rightarrow \gamma J/\psi$ $\hookrightarrow e^+e^-$
- $p\bar{p} \rightarrow \eta_c(2980) \rightarrow \gamma\gamma$

For each resonance, an excitation curve is constructed by changing the $\bar{p}$ beam momentum in appropriate steps. The error on the mass scale which depends on the knowledge of the $\bar{p}$ beam mean momentum is smaller than 0.3 MeV. The reconstructed J/ψ mass, $3096.95^{+0.14}_{-0.15}$ MeV, is in excellent agreement with previous measurements and provides another check of the mass scale.

The two χ states were identified by their decay to $\gamma J/\psi$. Their excitation curves are shown in Fig. 13; the shape results from the convolution of the beam profile and the χ Breit-Wigner. The $\chi(3510)$ line-shape, which is the mirror image of the beam profile, suggests a rather small width. The background, estimated by an off-resonance measurement, is negligible.

The results are given in Tab. 9. Using the Mark III measurement of $B(\eta_c \rightarrow p\bar{p})$, we deduce

$$B(\eta_c \rightarrow \gamma\gamma) = (3.9 \pm 4.0)10^{-4},$$

where the statistical and systematic errors have been combined quadratically.

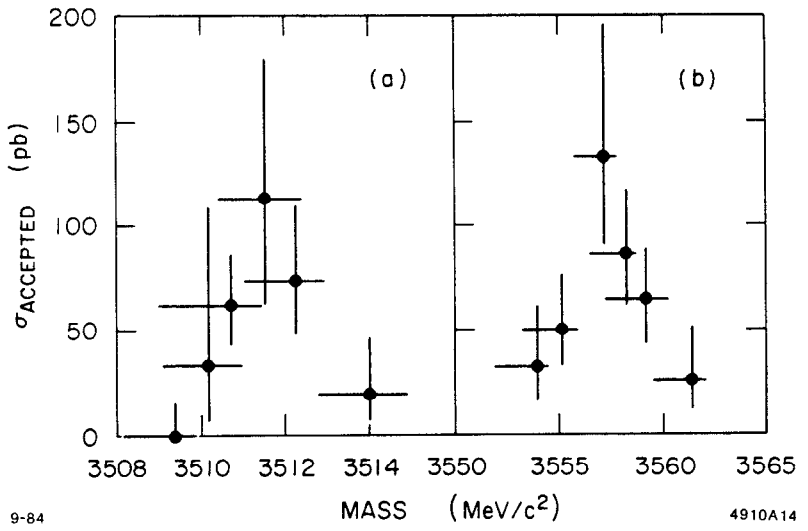

Figure 13. Excitation curve: a) $\chi(3510)$ b) $\chi(3555)$

Table 9. Preliminary results from R704.

Charmonium State	Mass (MeV)	$\Gamma(\chi \rightarrow p\bar{p})$ (eV)	$B(\eta_c \rightarrow p\bar{p}) \times B(\eta_c \rightarrow \gamma\gamma)$
$\chi(3510)$	$3511.4 \pm 0.3 \pm 0.4$	62 ± 15	
$\chi(3555)$	$3556.8 \pm 0.4 \pm 0.4$	208^{+75}_{-35}	
$\eta_c(2980)$			$(4.3 \pm 3.6)10^{-7}$

6. SUMMARY

The measurement of the $J/\psi \rightarrow$ Vector+Pseudoscalar branching ratios suggests that the light quark content of the η' is smaller than one, in contrast to that of the η.

The spin-parity of the $\iota(1440)$ and $\theta(1690)$ are now well established: 0^- for the iota and 2^+ for the theta.

There is evidence for the radiative decay $\iota(1440) \rightarrow \gamma\rho^0$ and for the $\theta(1690) \rightarrow \pi^+\pi^-$ decay mode.

Preliminary determinations of the $\chi(3510)$ and $\chi(3555)$ $p\bar{p}$ partial widths, and of the $B(\eta_c \rightarrow \gamma\gamma)$ branching ratio have been obtained.

ACKNOWLEDGEMENTS

I would like to thank K.F. Einsweiler, H.E. Haber, J.D. Richman, A. Seiden, A.L. Spadafora, and W. Toki for their help in preparing this talk, and R. Cester, C. Edwards, and G. Szklarz for fruitful discussions.

REFERENCES

1. S. Okubo, Phys. Lett., **5**, 165 (1963)
   G. Zweig, 1964 (unpublished)
   J. Iizuka, Prog. Theor. Phys. Suppl., **37-38**, 21 (1966)
2. In Rosner's notation (Phys. Rev. **D27**, 1101 (1983)), the meson wave function can be written

$$|\varphi\rangle = X_\varphi|N\rangle + Y_\varphi|S\rangle + Z_\varphi|G\rangle$$

   where the basis states are

$$|N\rangle = \frac{1}{\sqrt{2}}|u\bar{u} + d\bar{d}\rangle$$
$$|S\rangle = |s\bar{s}\rangle$$
$$|G\rangle \equiv |gluonium\rangle$$

   and

$$X_\varphi^2 + Y_\varphi^2 + Z_\varphi^2 = 1$$

3. The different amplitudes are calculated from the effective interaction lagrangian

$$\mathcal{L} = G \cdot V^a P_a + E \cdot d_{abc} S^a V^b P^c$$

   where V^a and P^a are the vector and pseudoscalar nonets, d_{abc} are the symmetric structure constants of SU(3), and S^a is a spurion field with the photon SU(3) transformation properties. G is the 3-gluon annihilation amplitude and E is the eletromagnetic amplitude, proportional to the quark magnetic moment μ.

The effect of the SU(3) breaking ($m_u = m_d \neq m_s$) on G is taken into account by the extra term

$$H \cdot d_{abc} S'^a V^b P^c$$

where S'^a transforms like the octet 8th component.

As $\mu \propto 1/m$, the electromagnetic contribution to a specific channel has to be corrected when strange quarks are involved. The calculation is straightforward and results in different multiplicative functions of $x = \mu_s/\mu_u$.

Finally, g, h and e are defined by

$$g = G + \frac{H}{\sqrt{3}}$$

$$h = \frac{\sqrt{3}}{2} H$$

$$e = \frac{E}{3}$$

See, for instance:
H. Kowalski and T.F. Walsh, Phys. Rev. **D14**, 852 (1976).
P. J. O'Donnell, Rev. Mod. Phys. **53**, 673 (1981).
N. Isgur, Phys. Rev. Lett. **36**, 1262 (1976).

4. In this calculation, a possible difference between the pseudoscalar form factors has not been taken into account.
5. A. De Rújula, H. Georgi and S.L. Glashow, Phys. Rev. **D12**, 147 (1975).
6. The partial width values were taken from:

- $\Gamma(\omega \to \gamma\pi^0)$, $\Gamma(\phi \to \gamma\eta)$, $\Gamma(\pi^0 \to \gamma\gamma)$ and $\Gamma(\eta \to \gamma\gamma)$: Review of particle properties, Rev. Mod. Phys. **56**, No. 2 part II (1984).
- $\Gamma(\rho^0 \to \gamma\eta)$: D. Andrews et. al., Phys. Rev. Lett. **38**, 198 (1977). There are two possible solutions. We used an average value with large errors.
- $\Gamma(\eta' \to \gamma\gamma) = (3.80 \pm 0.26 \pm 0.43)$ keV from PLUTO, Phys. Lett. **142B**, 125 (1984).
- $\Gamma(\eta' \to \gamma\rho^0)$ and $\Gamma(\eta' \to \gamma\omega)$ were calculated from the known η' branching ratios and its total width, (200 ± 34) keV, which was derived from $\Gamma(\eta' \to \gamma\gamma)$.

7. D. L. Scharre et al., Phys.Lett. **B97**, 329 (1980).
8. C. Edwards et al., Phys. Rev. Lett. **49**, 259 (1982).
9. J. E. Augustin et al., contributed paper to the XXII International Conference on High Energy Physics, Leipzig, July 19-25, 1984.
10. Review of particle properties, Rev. Mod. Phys. **56**, No. 2 part II (1984).
11. S. M. Berman and M. Jacob, Phys. Rev. **139B**, 1023 (1965).
12. See, for instance:
W. Palmer and S. Pinsky., Phys. Rev. **D27**, 2219 (1983).
C. Rosenzweig, proceeding of the MRST meeting, 1, (1982).
J. Donoghue, Phys. Rev. **D30**, 114 (1984).
T. Barnes and F.E. Close, RAL–84–055, (1984).
C. E. Carlson and T.H. Hansson, Nucl. Phys. **B199**, 441 (1982).
K. Senba and M. Tanimoto, Nuov. Cim. Lett. **35**, 295 (1982).

13. C. D. Edwards, CALT–68–1165, Ph.D. Thesis (1984).

14. W. Lockman, proceedings of the XVIII Rencontre de Moriond, La Plague, January 23-29, 1983.

15. M.E.B Franklin, Ph.D. Thesis, SLAC-254, (1982) (unpublished).

16. For a detailed discussion, see K.F. Einsweiler, Ph.D. Thesis, SLAC-272, (1984) (unpublished).

17. A 2^+ spin-parity were also preferred by the Crystal Ball analysis (C. Edwards et al., Phys. Rev. Lett. **48**, 458 (1982)). However, the possible presence of the $f'(1525)$ in the $\eta\eta$ channel was not taken into account.

18. CERN-R704, an Annecy-CERN-Geneva-Lyon-Oslo-Roma-Strasbourg-Torino Collaboration. For a detailed discussion of these results, see C. Baglin et al., CERN EP/el-0027P.